ICARUS 106, 380–391 (1993)

An Unusual Spectral Unit in West Candor Chasma: Evidence for Aqueous or Hydrothermal Alteration in the Martian Canyons

PAUL E. GEISSLER, ROBERT B. SINGER, AND GORO KOMATSU

Planetary Image Research Laboratory, Department of Planetary Sciences, University of Arizona, Tucson, Arizona 85721
E-mail: geissler@pirl.lpl.arizona.edu

SCOTT MURCHIE

Lunar and Planetary Institute, 3303 NASA Road 1, Houston, Texas 77058

AND

JOHN MUSTARD

Department of Geological Sciences, Brown University, Providence, Rhode Island 02912

Received February 5, 1993; revised August 20, 1993

High spatial-resolution observations made by orbiting spacecraft from the Viking and Phobos missions suggest the local development of crystalline ferric oxides in a small area in Mars' Valles Marineris canyon system. Quantitative color analysis of Viking Orbiter multispectral images identifies two spatially coherent regions of unique hue among the interior layered deposits in western Candor Chasma. The anomalous color indicates a local compositional difference between these regions and the surrounding high-albedo materials. The unusual appearance of the unit in the Viking color observations could be explained by a small increase in the degree of crystallinity or abundance of hematite. Near-infrared spectra obtained by the ISM imaging spectrometer aboard Phobos 2 confirm a local enrichment in ferric oxides or oxyhydroxides in the region and suggest the presence of another phase in addition to hematite.

In high resolution, the spectral unit can be seen to occur within two 20-km-long depressions on the margins of an Hesperian-aged layered deposit which forms a plateau on the chasma floor. Water is implicated in the formation of the iron oxides, since the same sedimentary layers seen in the depressions are exposed on steep surfaces elsewhere on the plateau but show no evidence of unusual coloration. This suggests that the mineralization occurred through secondary alteration of preexisting rocks and developed locally in association with the depressions, which could have ponded surface runoff or groundwater seepage.

1. INTRODUCTION

Previous Earth-based observations (reviewed by McCord and Adams 1969, Singer 1985, and Soderblom 1992, among others) have long established the presence of two major spectral components on Mars. Classical low-albedo regions show the signature of a relatively pristine mafic or ultramafic composition distinguished by Fe^{2+} absorption bands and a blue (slightly negatively sloping) IR continuum (Adams and McCord 1969, McCord and Wesphal 1971, Binder and Jones 1982, Singer 1980, Singer and McSween 1993). High-albedo areas and optically thick dust storms have a characteristic orange-red color believed to be due to more heavily oxidized ferric (Fe^{3+}) iron mixed with spectrally neutral material (e.g., Huguenin *et al.* 1977; Singer 1982). Although crystalline ferric oxides such as hematite (αFe_2O_3) or maghemite (γFe_2O_3) should be thermodynamically stable in the present martian environment (Berner 1969, Gooding 1978), in general the ferric iron component is thought to be very finely crystalline (nanophase) or poorly crystalline. This is because even small quantities of coarsely crystalline hematite show distinctive absorption bands in visible and near infrared wavelengths which are absent from or very weak in the spectra of Mars' bright regions (Singer 1982, Singer and Miller 1991, Bell *et al.* 1990, Bell 1992). The failure of oxidation to equilibrate and produce crystalline ferric oxides as weathering products is thought to be due to limitations of chemical kinetics caused by the low temperature and lack of moisture on Mars (Banin 1992, Gooding *et al.* 1992, Burns and Fisher 1993).

With increasing spatial resolution, reflectance spectroscopy is beginning to provide the capability to study compositional variation on the surface of Mars in more detail than was previously possible. High-spatial-resolution spectral images obtained during the 1988 opposition by Earth-based observers Singer and Miller (1991) and Bell *et al.* (1990, 1992) show regional areas in which crystalline

0019-1035/93 $5.00

ferric oxides are sufficiently enriched to be spectroscopically observed. Recent observations by the orbiting spacecraft Phobos 2 similarly show evidence of spectral heterogeneity at wavelengths indicative of ferric oxides (Murchie *et al.* 1993). These may be regions where variations in primary composition or in the local chemical or thermal environment have allowed oxidation reactions to proceed further toward equilibrium.

In this paper we report on high-spatial-resolution observations made by orbiting spacecraft from the Viking and Phobos missions, which suggest the local development of crystalline ferric oxides in a unique area in Mars' Valles Marineris canyon system and suggest possible geologic interpretations based upon terrestrial analogs.

2. SPECTRAL IMAGING OBSERVATIONS

2.1. Viking Color

The Viking Orbiter Visual Imaging Subsystem (VIS) produced a wealth of color data at high spatial resolutions using two vidicon cameras equipped with filter wheels on each of the two Orbiters (Thorpe 1976, Klaasen *et al.* 1977). Most of the surface of Mars was imaged in the red (0.59 μm), green (0.53 μm), and violet (0.45 μm) bandpasses. Later, in the extended or Survey mission of Viking Orbiter 1, images were obtained only in red and violet—also the choice for the Mars Observer Camera (Malin *et al.* 1992) as sufficient for distinguishing surface features from clouds.

A standard technique (e.g., Gillespie *et al.* 1986) for analyzing three-color data is rotation to hue, saturation, and intensity coordinates to identify relationships between the three-point spectra of various surface units. Using a computer program developed by E. Merenyi (University of Arizona), Viking apoapsis images of the Valles Marineris region were analyzed in this way after radiometric calibration using procedures made available by the Astrogeology Branch of the U.S. Geological Survey (USGS 1988). The relative uncertainty (across a single image) for calibrated Viking images is estimated to be less than 3% (Klaasen *et al.* 1977). The violet, green, and red filter images were coregistered to form composites and the set of radiance factors (v, g, r) for each pixel was used to compute a corresponding hue H, saturation S, and intensity I, where

$$H = \operatorname{acot}\left[\frac{\sqrt{3}\,(v-r)}{v-2g+r}\right]$$

$$S = \operatorname{acos}\left[\frac{v+g+r}{\sqrt{3(v^2+g^2+r^2)}}\right]$$

$$I = \text{maximum}\,(v, g, r).$$

In general, the visible spectra of bright materials in Coprates Quadrangle were found to be simply related by multiplicative and additive effects, suggesting that physical rather than compositional differences dominate the spectral variations among high-albedo materials (Geissler 1992, Geissler and Singer 1992). However, a spectrally anomalous bright region is identified in the color decomposition results shown in Fig. 1, produced from low phase angle (20°) red, green, and violet images acquired in January 1978 by Viking Orbiter 1 on orbit 583. Figure 1b shows the intensity or "value" component, essentially equivalent in the present application to the red filter image. Figure 1c is the saturation image, in which materials with spectra related by a simple multiplicative scaling appear the same. Figure 1d shows the hue of the region; two areas will have the same hue if their spectra are related by a linear transformation of the form

$$r'(\lambda) = a_0 + a_1 r(\lambda),$$

where $r(\lambda)$ is the spectral reflectance and a_0 and a_1 are constants.

Most distinctions between bright materials disappear in this hue image, but an exception occurs in West Candor Chasma where two spatially coherent regions are noticeably redder than the environs (numerals in Fig. 1a; also Fig. 2). West Candor Chasma (centered at 6°S, 76°W) lies in the geologically complex central troughs of the Valles Marineris, a set of short, blunt chasmata trending parallel to the main Ius–Coprates canyon system in which volcanism, tectonism, deposition, and erosion have been interpreted (Lucchita 1990, Witbeck *et al.* 1991, Lucchitta *et al.* 1993). The unit occurs on the flanks of a freestanding mesa on the chasma floor which is interpreted to be a layered sedimentary deposit of Hesperian age (Nedell *et al.* 1987, Witbeck *et al.* 1991), but which appears spectrally and morphologically distinct from layered deposits elsewhere in the Valles Marineris (Komatsu *et al.* 1993, McEwen 1992). The anomalous color of the unit is due to a reduced green filter reflectance, relative to violet and red, in comparison to surrounding materials of similar albedo or average reflectance. Unlike most spectral variations among bright materials in this region, the coloration is not the result of wavelength-independent effects (such as mixing with or induration by spectrally neutral materials). Instead, this hue anomaly indicates a local compositional difference.

The presence of clouds and possible surface frosts in image 583A prompted us to examine other color imaging sequences to determine whether the unusual color was a permanent feature of the surface. The region was imaged again by Viking Orbiter 1 4 months later during orbit 701, and the distinct coloration is evident despite the higher

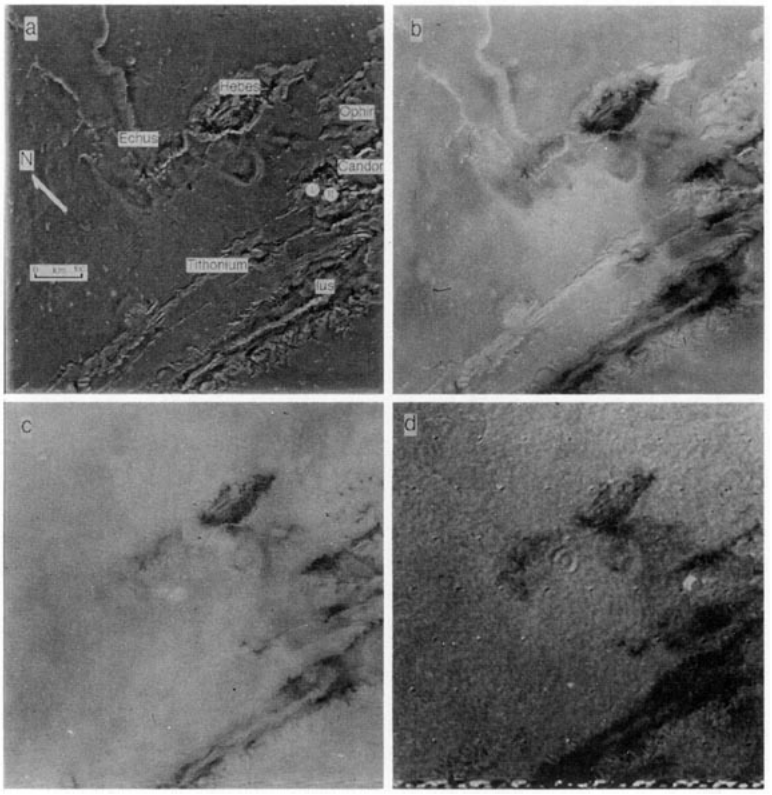

FIG. 1. Color decomposition, orbit 583A. Viking Orbiter 1 image from orbit 583, centered at 3° S, 80° W. This three-color composite has been separated into components: (b) intensity, (c) saturation, and (d) hue. A grid of incompletely removed reseau marks is seen in the hue image, as is a dust particle diffraction ring near the center. Low-albedo markings on the plains west of Echus which are visible in the intensity and saturation images disappear in the hue image. Two small regions in West Candor Chasma (numerals) are redder than the nearby canyon walls and floor covering materials, which are similar in hue to the plains.

phase angle (53°). Early in the mission of Viking Orbiter 1, a very high phase angle (109°) sequence taken on orbit 40 partially covers the strongly colored northern exposure ("1" in Fig. 1a), which again appears redder than the nearby canyon walls. The West Candor regions do not, however, appear distinctive in the Survey Mission data (orbit 334S) which was acquired without the compositionally important green filter.

The highest-resolution three-color composite of the area was obtained by Viking Orbiter 2 on orbit 279 in May 1977 at a phase angle of 57°. Figure 2c shows this oblique view of Western Candor Chasma from the South at a spatial resolution of 240 m/pixel. The unusual spectral unit can be seen to correspond to two depressions on the margins of a heavily eroded plateau-forming deposit on the canyon floor which we unofficially call "Red Mesa." The northern depression, in which the coloration is best developed (cf. Fig. 2a), is almost 20 km in length. Another, somewhat less distinct, exposure corresponds to the "toe" of the boot-shaped depression on the eastern edge of the mesa. To the south, near the summit of Red Mesa, a high-albedo region with notably sinuous margins does not show evidence of the unusual coloration.

Figure 3 compares the three-point Viking spectrum of the anomalous region to those of neighboring bright materials with similar green-filter reflectance in order to characterize the distinctive color of the unit. Both the violet and the red filter reflectance values are larger than ex-

FIG. 2. Spectrally anomalous unit in West Candor Chasma. (a) The unique color of the West Candor unit is noticeable in this composite from orbit 583A, which has been enhanced so that relatively gray materials appear blue. Image centered at 5°S, 76°W; picture width is about 375 km; north is toward the top left. (b) Hue component derived from image 583A. This is an enlarged portion of Fig. 1d. (c) Highest-resolution three-color composite of the West Candor Chasma area. Acquired on orbit 279B, this enhanced color image is an oblique view from the south at a spatial resolution of 240 m/pixel. The ususual spectral unit can be seen to correspond to two depressions on the margins of "Red Mesa," a heavily eroded plateau-forming deposit in the chasma interior. Picture width is about 75 km; north is toward the top left.

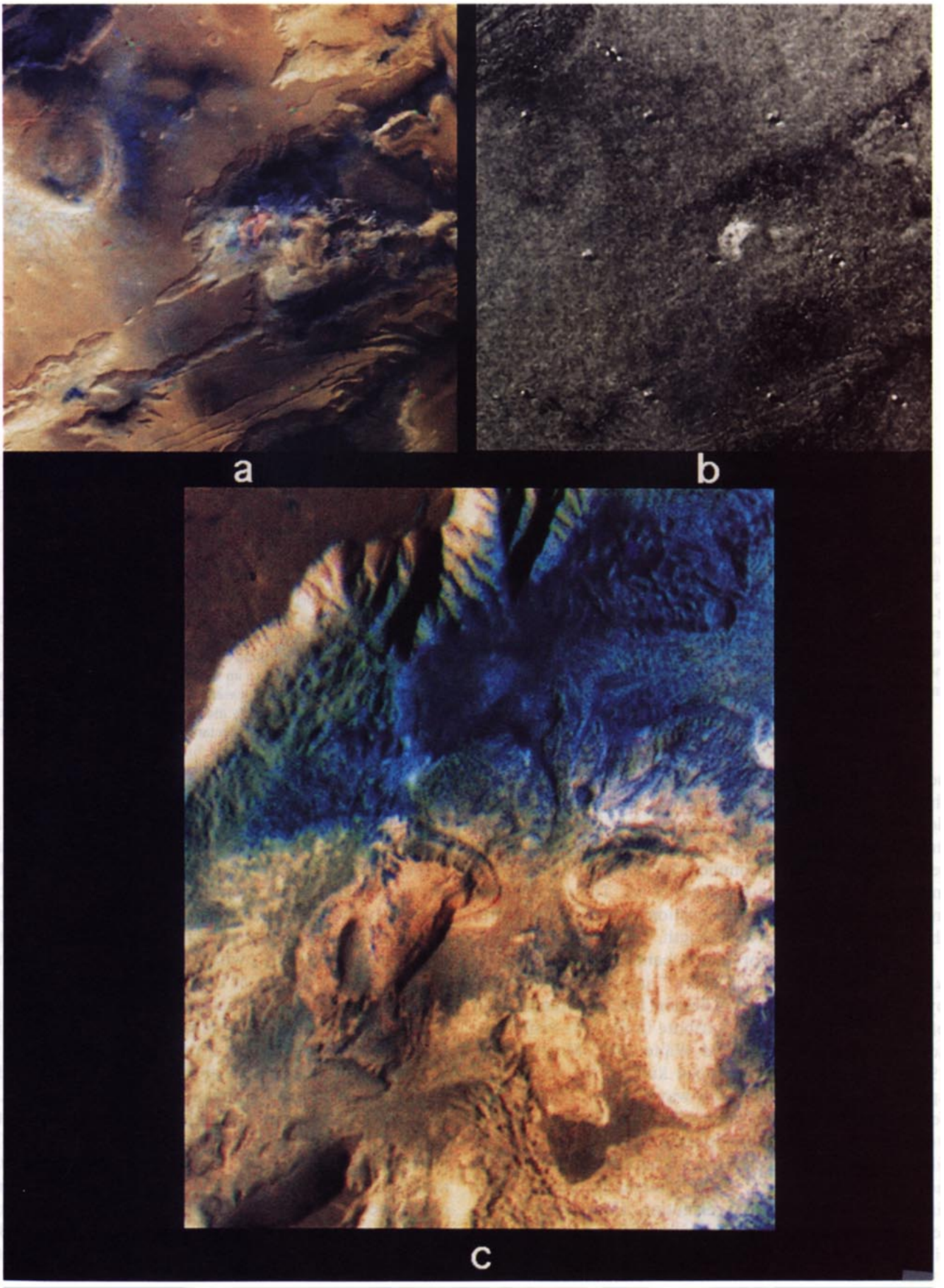
a
b
c

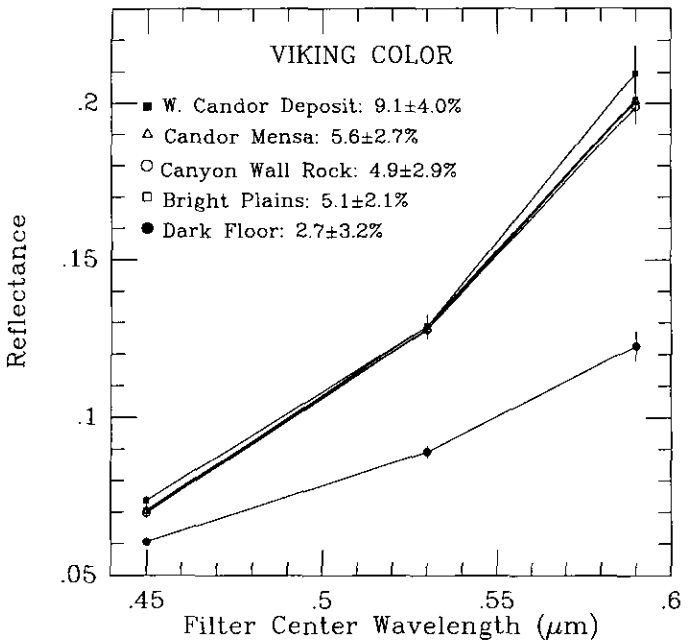

FIG. 3. Three-point Viking spectra. The color of the anomalous region differs only slightly from those of neighboring bright materials with similar green-filter reflectance including canyon wall rock, nearby plains units and more typical layered deposits found in Ophir Chasma to the East. The difference is made apparent by the values listed for $(1\text{-}k)$, a measure of the depth of an absorption band coinciding with the green filter center wavelength (see text). Quoted uncertainties and error bars are based on the standard deviation within each 40- to 72-pixel box measured. Also shown for reference is the spectrum of a typical dark unit from the chasma floor north of Red Mesa.

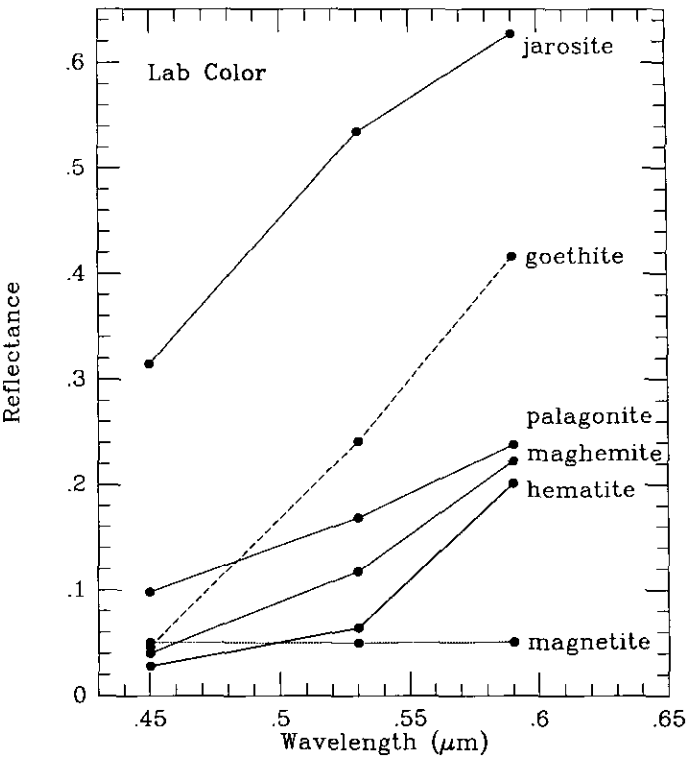

FIG. 4. Laboratory observations at Viking spectral resolution. A suite of potential Mars-analog materials are shown as they would appear through the Viking Orbiter bandpasses. Despite their limited spectral range and resolution, the Viking color data can be diagnostic of specific iron oxide mineralogy, due to an absorption band of Fe^{3+} in hematite at 0.53 μm. Hematite and, to a lesser extent, its cubic polymorph maghemite are distinctive among likely martian materials in displaying a kink due to depressed green filter reflectance. Spectral measurements from R. B. Singer.

pected for the unit's green filter reflectance; alternatively, the green filter reflectance of the West Candor unit is depressed relative to the red and violet filter values. The unit is noticeable in red/green ratio images, indistinct in red/violet ratios, and prominent in "kink" or band-depth images constructed as $k = 2g/(r + v)$. The parameter k measures the depth of an absorption band coinciding with the green filter center wavelength.

A likely candidate for such a band is the strong 0.53-μm crystal field transition of Fe^{3+} in hematite, as noted by Sherman *et al.* (1982) and Singer (1982). A combination of electronic transitions contribute to the UV–visible absorption edge (Sherman and Waite 1985, Morris *et al.* 1985), producing a pronounced kink in the reflectance spectrum of hematite at visible wavelengths. This spectral feature is retained even when reflectance spectra are convolved to the spectral bandpasses of the broadband VIS filters (Fig. 4). In this case the Viking color data are diagnostic of specific ferric oxide mineralogy despite their limited spectral range and resolution. Hematite and, to a lesser extent, its cubic polymorph maghemite are distinctive among likely martian analogue materials in displaying a kink due to depressed green filter reflectance. As this spectral feature appears common in the observed surface colors (Fig. 3), it is likely that trace quantities of hematite are ubiquitous among the rocks and soils of the central Valles Marineris. The color anomaly found in West Candor Chasma may be due to local enrichment of hematite (i.e., "mineralization") within the depressions. A small increase in the degree of crystallinity or abundance of hematite could explain the greater band depth and unusual appearance of the Red Mesa depressions in the Viking Orbiter color observations. If that were the case, then we should expect an enhanced absorption in the near-IR due to the $^6A_1 \rightarrow {}^4T_1$ band of hematite at 0.87 μm as well.

An opportunity to test this hypothesis was presented by data from the Imaging Spectrometer for Mars (ISM) instrument on Phobos 2. Figure 5 shows the spectral ranges of the Viking VIS and the short wavelength second-order spectra from ISM, superimposed on a laboratory spectrum of reagent-grade hematite from Singer (1982). Over the wavelength range observable from ISM, the

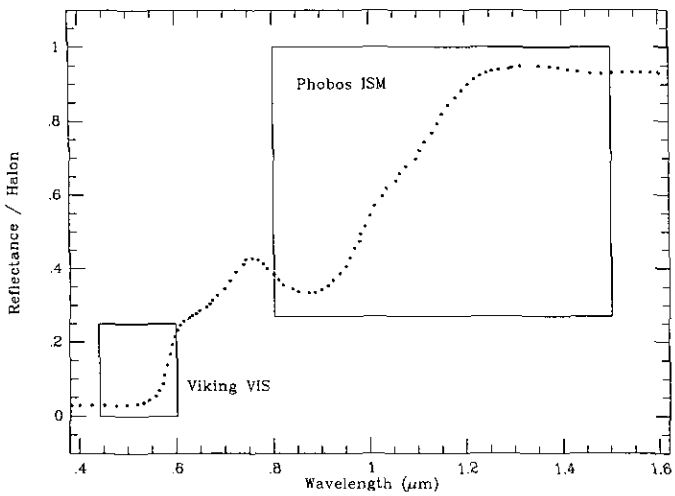

FIG. 5. Hematite spectrum. Spectral ranges of the Viking VIS and the short wavelength second-order spectra from ISM are shown superimposed on a laboratory spectrum of reagent-grade hematite from Singer (1982).

reflectance spectrum of hematite reaches a minimum due to the aforementioned band at 0.87 μm and rises to a nearly constant continuum reflectance between 1.2 and 1.4 μm.

2.2. *Phobos ISM Observations*

Over 36,000 high-spatial-resolution infrared reflectance spectra of selected regions of Mars were obtained by the imaging spectrometer ISM on the Russian probe Phobos 2 in 1989 (Bibring *et al.* 1989, 1990). Two spectral ranges corresponding to the first order (1.64–3.16 μm) and the second order (0.76–1.51 μm) of the diffraction grating comprise these data. Initial calibration for instrumental and atmospheric effects, including removal of CO_2 absorption features, was described by Erard *et al.* (1991). Calibration of the short-wavelength second-order spectra used here was refined be calculating gain and offset corrections based on low- and high-albedo standard areas and telescopic spectra in order to reduce residual systematic errors (Mustard *et al.* 1993). Slightly different areas of the surface are imaged by the even- and odd-numbered channels of each detector array, so the least uncertainty is achieved by considering a subset of 32 of the available 64 detectors within each order. The absolute-radiometric accuracy of a given ISM channel is estimated to be around 10%, but the relative uncertainty (relevant when comparing one spectrum to another) is less than 1% for the wavelength range examined here (Erard *et al.* 1991).

A single pixel spectrum from the even-numbered channels of the second-order ISM data, corresponding to the location of the uniquely colored depression in West Candor Chasma, is shown in Fig. 6 along with a spectrum from the brighter and more typically hued surface of Red Mesa just south of the unusual exposure. Also shown in a four-pixel average recorded from Ophir Planum plains north of East Candor Chasma, a spatially uniform region typical of bright martian soils, and a single-pixel spectrum from the dark fractured floor in central Candor Chasma which is representative of pyroxene-bearing, relatively unoxidized mafic materials. Band depths for each of these spectra were computed by dividing the minimum reflectance in the wavelength interval from 0.8 to 1.0 μm by the mean reflectance in the continuum wavelength range from 1.2 to 1.4 μm. We have chosen this method of computation because the available data do not cover the short-wavelength end of the absorption bands of interest; however, qualitatively similar results are obtained when the continuum reference level is taken to be the mean of the reflectance values at 0.774 and 1.090 μm. Despite the fact that the exposure does not completely fill the 22 $\times$

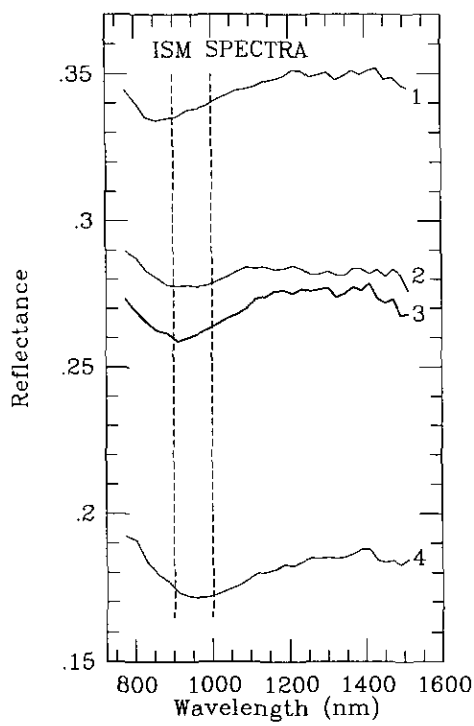

FIG. 6. ISM Spectra. A single pixel spectrum from the even-numbered channels of the second-order ISM data, corresponding to the location of the uniquely colored depression in West Candor Chasma (3), is shown along with a spectrum from the brighter and more typically hued slopes of Red Mesa just south of the unusual exposure (2). Also shown is a four-pixel average recorded from the Ophir Planum bright plains north of East Candor Chasma (1), a spatially uniform region typical of bright martian soils, and a single-pixel spectrum from the dark fractured floor in central Candor Chasma which is representative of pyroxene-bearing, relatively unoxidized mafic materials (4). Band depths, computed as 1.0 − (reflectance at band minimum/average reflectance in 1.2–1.4-μm interval), are as follows: (1) 4.6%; (2) 1.9%; (3) 6.4%; (4) 7.5%.

22-km footprint of an ISM pixel, these data show an enhanced absorption near 0.91 μm for the mineralized depression with a band depth (6.4%) more than 3 times greater than the adjacent unmineralized layered deposits (1.9%). For comparison, a maximum band depth of 4.6% for the Ophir Planum bright soil is reached at a wavelength of 0.87 μm, diagnostic of hematite, while the pyroxene-rich dark materials have a band depth and center of 7.5% at 0.96 μm.

We interpret these observations to indicate a greater local development of crystalline ferric oxides within the Red Mesa depression, in comparison to the adjacent unmineralized surface of Red Mesa to the South. Establishing the precise mineralogy is complicated by instrumental noise in a channel critical to determination of the band centers (0.884 μm). Nevertheless, the apparent 0.9-μm center wavelength of the band suggests that the mineralization is unlikely to consist of hematite alone, even though the visible color of the unit is very likely dominated by hematite. Although grain-size effects and substitution of other cations such as Al for Fe can shift the hematite 0.87-μm band center wavelength longward to a limited extent (Morris *et al.* 1985, 1992), the band center determination from ISM seems to require an additional phase. One possibility is mixing of ferrous (Fe^{2+}) and ferric (Fe^{3+}) iron spectral signatures. Laboratory measurements (Bell and Morris, *personal communication* 1993) suggest that subequal mixtures of hematite and pigeonite pyroxene can produce an unresolved composite absorption band with a center wavelength intermediate between the 0.87-μm band center of hematite and the 0.95-μm wavelength of pigeonite. Pyroxene is known to be an important constituent of martian rocks and soils, and very likely contributes to the broad, shallow absorption band in the spectrum of the unmineralized Red Mesa layered deposits adjacent to the degressions (spectrum 2 in Fig. 6). However, the *difference* between the spectra of the uniquely hued depressions and the layered deposits in which they occur reaches a maximum at 0.9 μm rather than 0.87 μm (Fig. 7). This would not be the case if the enhanced absorption band were an unresolved doublet due to mixing of ferrous iron with hematite. Another interesting possibility is shown in Fig. 8, from Townsend (1987). Many hydrated or hydroxylated Fe^{3+} minerals such as goethite, jarosite, and ferrihydrite have deep absorption bands centered near 0.9 μm (Morris *et al.* 1985, Townsend 1987). These minerals are not currently stable in the martian environment, and their paragenesis on Earth generally involves contact with liquid water. Although the data are by no means conclusive, the combined visible and near-infrared spectral evidence for the composition of the Red Mesa anomaly suggests a mixture of hematite with hydrated or hydroxylated Fe^{3+} minerals, an interpretation with important implications for the genesis of the mineralization.

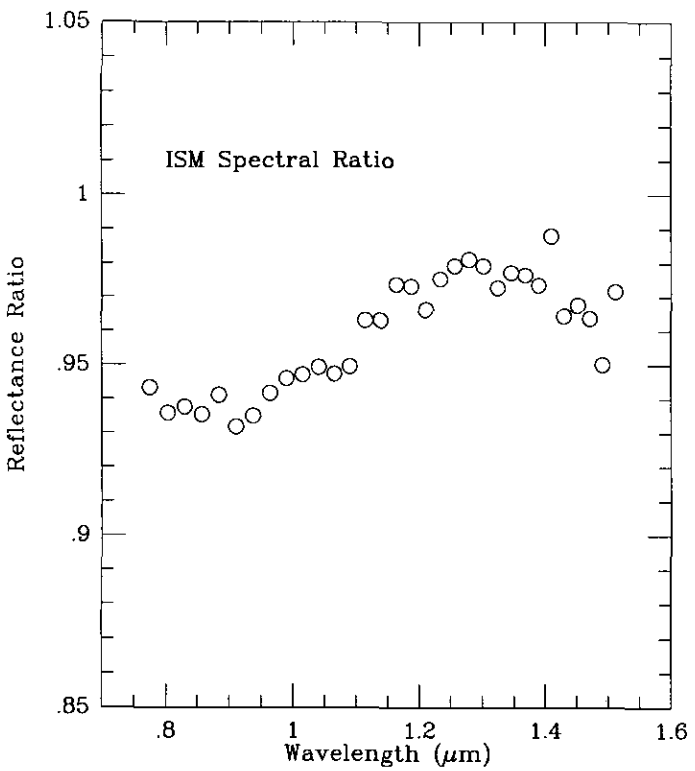

FIG. 7. *ISM spectra ratio.* The ISM spectrum from the uniquely colored depression (spectrum 3 in Fig. 6) has been divided by the spectrum from the adjacent layered deposits (2 in Fig. 6) to better show the difference between the spectral signature of the mineralization and the unaltered host rock in which it occurs. A contaminant with a broad absorption band centered near 0.9 μm appears to comprise the mineralization.

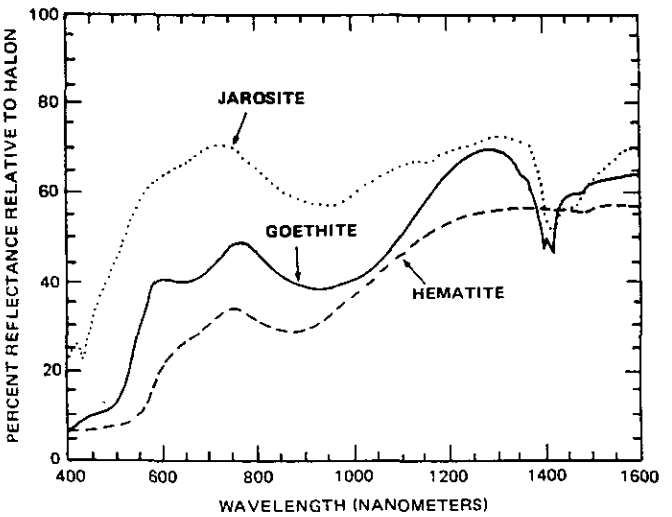

FIG. 8. Spectra of several ferric oxides compared. Goethite and jarosite, two hydroxylated ferric oxides, both have absorption bands centered near 0.9 μm (from Townsend, 1987).

3. GEOMORPHOLOGY

Figures 9 and 10 show the topography and high-resolution morphology of Western Candor Chasma. The trough is dominated by a large, plateau-forming layered deposit (Red Mesa) rising more than 6 km above the canyon floor. Surrounding Red Mesa are young, mottled floor-covering deposits which postdate both the layered sediments and even some avalanche deposits produced by relatively recent landslides from the canyon walls (Lucchitta 1990). Laminae (marked "L" in Figure 10) are conspicuous in several places on the plateau. These are probably depositional layers, but some may be erosional benches instead (Komatsu *et al.* 1992). The layering is particularly evident within the mineralized depression at the northern margin of Red Mesa where 15 to 20 cycles of alternating bright and dark layers are exposed at approximately 200-m vertical intervals. Nearby layers on the steep, vertically fluted cliffs to the south of this depression (Figure 10) are presumed to be continuous with the strata in the mineralized zone, respresenting the same depositional horizons although displaying none of the distinctive coloration seen within the depressions. Concentric markings ("Lc" in Figure 10) indicate a basin in the depression on the eastern margin of Red Mesa at the location of the less pronounced hue anomaly (the toe of the boot; cf. Fig. 2). The sinuous morphology of the cap rock ("C") at the summit of Red Mesa is probably due to uneven erosion, exposing a bright layer at the top.

Lineations and apparent structural control of topography suggest tectonic activity in West Candor Chasma. East–west-trending graben, catena (crater chains), and steep canyon walls parallel to the main Tithonium–Coprates canyon system to the south are consistent with the general tectonic pattern of extensional faulting radial to the Tharsis Rise (Plescia and Saunders 1982). The southern part of the west margin of Candor Chasma is also markedly linear, with a northeasterly trend which can be followed along a direct line to reach the anomalously colored zone at the northern margin of Red Mesa. A distinct lineation at the base of this scarp ("F" in Fig. 10) transects mottled canyon floor deposits believed to be among the youngest in the Valles Marineris (Lucchitta 1990). We interpret these observations to suggest that

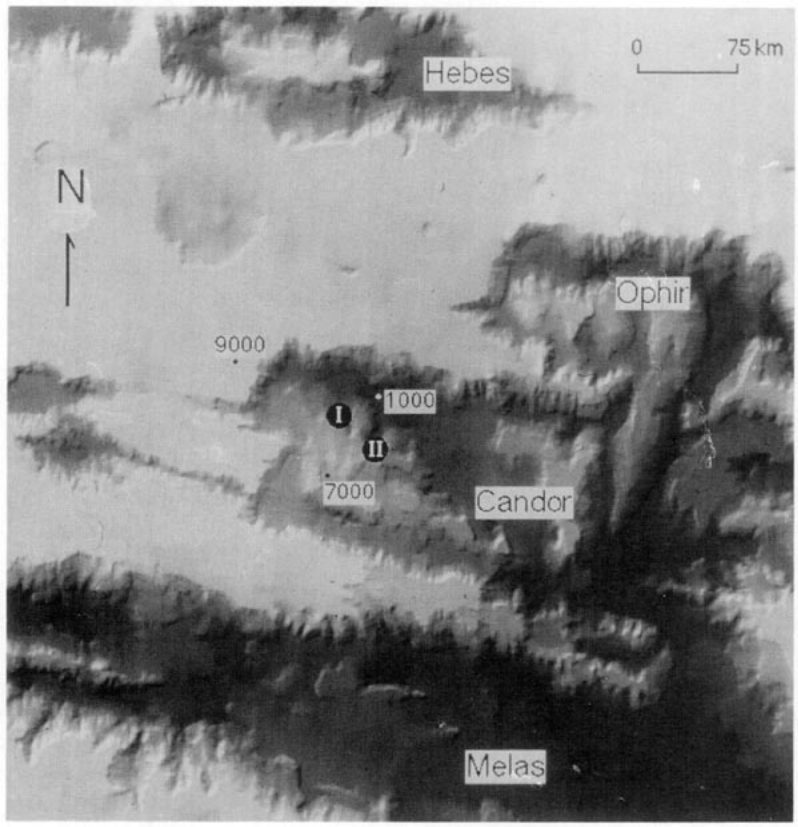

FIG. 9. Topography of Western Candor Chasma. Portion of the USGS Digital Terrain Model (DTM) of Mars (from Planetary Data System CD VO_2007), centered on 5°S, 76°W. The DTM has been rendered such that the surface appears to be illuminated from the northwest. Numerals show the locations of the Red Mesa depressions. Spot elevations are in meters above the 6.1-mbar datum; the summit of Red Mesa is located near the 7000-m spot elevation.

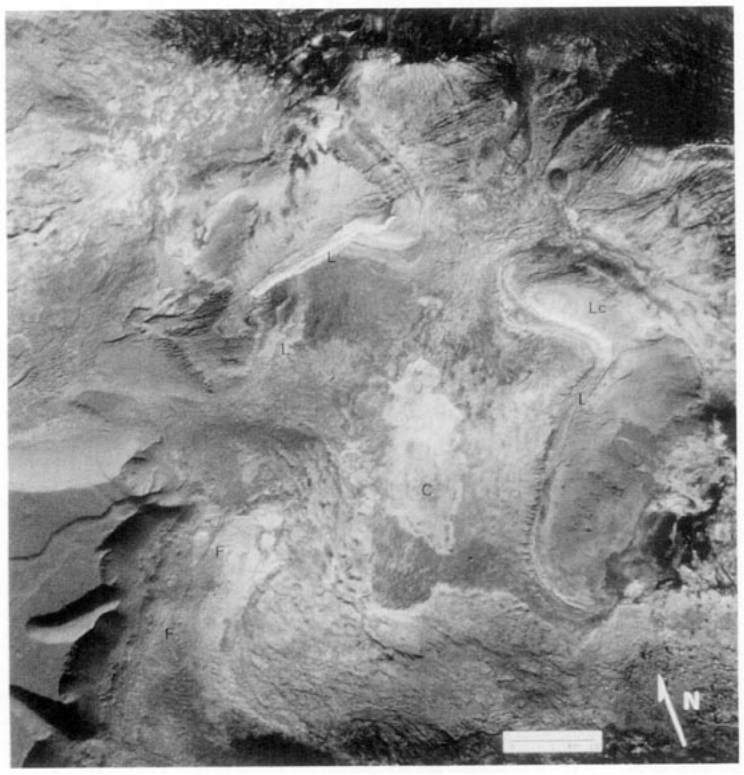

FIG. 10. Morphology of Western Candor chasma. Layers (marked "L") are conspicuous in several places on the plateau, particularly within the mineralized depression at the northern margin of Red Mesa and on the steep, vertically fluted cliffs to the south. Concentric markings ("Lc") indicate a basin in the depression on the eastern margin of Red Mesa at the location of the less pronounced hue anomaly (the toe of the boot; cf. Fig. 2). High albedo cap rock ("C") tops the plateau. A distinct lineation ("F") at the base of the scarp at the western end of the canyon transects mottled canyon floor deposits believed to be among the youngest in the Valles Marineris.

both the steep western rim of Candor Chasma and the mineralized depression peripheral to Red Mesa may be influenced by the presence of a major northeast–southwest trending fault, along which movement may have occurred in the relatively recent past.

4. DISCUSSION: ORIGIN OF THE MINERALIZATION

Several questions are raised by the interpretation of the spectral indications of a localized zone of enrichment of ferric oxide minerals. Under what circumstances did the mineralization form? Are we seeing evidence of compositional variation at the time of deposition, or the product of subsequent weathering or alteration?

On Earth, concentrations of iron oxides are formed through a variety of geologic processes. Hematite is a major component of many "gossans" (supergene ore deposits), long sought after by prospectors as indicators of weathering of near-surface orebodies. Ferruginous sandstones and laterites (iron-cemented soils common in tropical regions) are familiar examples of oxidation and precipitation of dissolved iron by surface- or groundwater. Sedimentary "limonite" is often a mixture of poorly crystalline hematite, goethite, and hydrated iron oxides; fluid temperature, pH, and oxygen fugacity determine the mineralogic makeup of the precipitate (see Schwertmann and Taylor 1989 for a recent review). Volcanism is another geologic process which produces local concentrations of hematite, as oxidation rinds on basaltic rocks and cinders, for example, or as hematitic soils produced by a combination of water and heat in regions of hydrothermal alteration.

Although attractive, a gossan-forming primary iron ore concentration is the least likely possibility for the mineralized zones in West Candor Chasma. The same sedimentary layers seen in the depressions are exposed on steep surfaces elsewhere on Red Mesa but show no evidence of unusual coloration. This suggests that (1) the mineralization is secondary in nature, and (2) it developed locally in association with the depressions. Based on Viking Lander analyses (Clark *et al.* 1982) which show a large Fe component in the martian fines, it is probable that iron was abundant in the sediments at the time of deposition and could have subsequently been converted to hematite by any of a variety of mechanisms ranging from thermal metamorphism to low temperature aqueous alteration.

Detailed knowledge of the mineralogy is important for constraining the conditions of formation of the deposit: simple heating under anhydrous conditions, which could have occurred if the depressions were volcanic calderas, for example, should produce Fe^{3+} mineralization which is dominantly or exclusively hematitic in composition. The interpreted presence of additional hydrated or hydroxylated ferric oxide phases, if confirmed, would argue for aqueous or hydrothermal alteration as the mechanism of origin for the mineralized zones.

Water is also implicated by the association of the mineralization with basins and depressions which could have ponded surface runoff or groundwater seepage. One likely scenario would have iron dissolved and leached from saturated sediments and precipitated as crystalline ferric oxides, perhaps forming an exotic martian evaporite. The interpretation of relatively recently developed paleolakes in ancient sedimentary deposits raises some interesting and as yet unanswered questions. How did the basins form? What was the source of the water? Rainfall runoff seems unlikely so late in martian history, and no direct evidence for recent fluvial modification has so far been identified tin the Central Troughs. However, morphological criteria for groundwater seepage have been noted by several workers (Sharp 1973, Soderblom and Wenner 1978, Kochel and Piper 1986), providing a plausible alternative mechanism for filling the "lakes" of West Candor Chasma.

Another important question is the role of heat in the formation of the deposits, particularly as thermal effects are important to the formation of hematite. Extensive, possibly recent volcanism has been proposed for this region (Lucchitta 1990). The proximity of a major fault in apparent association with the northern depression suggests the possibility of magmatic activity or circulating hydrothermal fluids along the plane of crustal weakening, perhaps providing a source of heat enabling oxidation reactions to more efficiently proceed to equilibrium. Heating may have played a part in the more extensive development of mineralization in the northern depression, in comparison to the basin on the eastern margin of Red Mesa. Geothermal heating could also have supplied water for filling the depressions through melting of ground ice.

A spectulative but intriguing question is raised by the inference of the involvement of water and/or heat in the formation of the mineralization in West Candor Chasma. Previous workers (e.g., Sharp 1973, Nedell *et al.* 1987) have discussed the possibility that large areas of the Valles Marineris were at one time filled with standing bodies of water and suggested a lacustrine origin for the interior layered deposits. However, the unusually colored depressions must have formed much later, after the layered deposits were exhumed and partially eroded. If surface water was in fact ponded in the small West Candor depressions, then they were probably among the last of such lakes in the Valles Marineris. The region may therefore be an interesting prospect for exobiologists, since the factors that favored the formation of ferric oxides within the depressions—namely water and warmth—are also conditions conducive to the development of life.

Future spacecraft exploration may shed some light on the origin of these enigmatic mineralized zones. The instrument complement incorporated in the Mars Observer mission remains particularly well suited to this goal. High-resolution imaging might show evidence of terraces or strand lines to support the interpretation of standing bodies of whater within the depressions. Precise altimetry would yield information about the detailed topography of the region, while ferric mineralogy and, significantly, possible clay mineral components should be identifiable by thermal emission spectroscopy. The iron mineralogy of this and other regions on Mars may be more fully constrained through further visible and near-infrared observations by a series of Russian spacecraft planned for the latter part of the decade (Barsukov, 1992).

5. SUMMARY

1. Quantitative color analysis of Viking Orbiter multispectral images identifies two spatially coherent regions of unique hue among the Hesperian layered deposits in the central Valles Marineris. Unlike most spectral variations between bright materials in this region, this coloration is not the result of wavelength-independent effects. Instead, it indicates a local compositional difference.

2. The reduced green-filter reflectance responsible for the anomalous color of these regions is probably caused by local enrichment of crystalline ferric oxides, particularly hematite.

3. Near-infrared spectra from the Phobos 2 ISM instrument are also consistent with an interpretation of elevated abundances of crystalline Fe^{3+} minerals in these areas. The absorption band center wavelength as determined from ISM data suggests that hydrated or hydroxylated ferric oxide minerals are present in the mineralized zone.

4. Geochemical arguments and morphological evidence suggest that water, heat, or a combination of both produced the mineralization by secondary alteration of the sediments in the geologically recent past. The region is therefore of much interest for intensive observation by impending future missions to Mars.

ACKNOWLEDGMENTS

The authors thank reviewers James Bell and Baerbel Lucchitta for their many valuable suggestions. This work was supported by NASA Grant NAGW-1059.

REFERENCES

ADAMS, J. B., AND T. B. MCCORD 1969. Mars: Interpretation of spectral reflectivity of light and dark regions. *J. Geophys. Res.* **74,** 4851–4856.

ALBEE, A. L., R. E. ARVIDSON, AND F. D. PALLUCONI 1992. Mars Observer mission. *J. Geophys. Res.* **97,** 7665–7680.

BANIN, A. 1992. *The Mineralogy and Formation Processes of Mars Soil.* Workshop on Chemical Weathering on Mars, Lunar and Planetary Institute Technical Report 92-04, Part 1, pp. 1–2. [Abstract]

BARSUKOV, V. I. 1992. Plans of future Russian planetary missions. *Bull. Am. Astron. Soc.* **24,** 977–978. [Abstract]

BELL, J. F., T. B. MCCORD, AND P. D. OWENSBY 1990. Observational evidence of crystalline iron oxides on Mars. *J. Geophys. Res.* **95,** 14447–14461.

BELL, J. F. 1992. Charge coupled device imaging spectroscopy of Mars. 2. Results and implications for martian ferric mineralogy. *Icarus* **100,** 575–597.

BERNER, R. A. 1969. Goethite stability and the origin of red beds. *Geochem. Cosmochem. Acta* **33,** 267–273.

BIBRING, J.-P., M. COMBES, Y. LANGEVIN, A. SOUFFLOT, C. CARA, P. DROSSART, TH. ENCRENAZ, S. ERARD, O. FORNI, G. GONDET, L. KSANFOMALITY, E. LELLOUCH, PH. MASSON, V. MOROZ, F. ROCARD, J. ROSENQVIST, AND C. SOTIN 1989. Results from the ISM experiment. *Nature* **341,** 591–593.

BIBRING, J.-P., M. COMBES, Y. LANGEVIN, C. CARA, P. DROSSART, TH. ENCRENAZ, S. ERARD, O. FORNI, G. GONDET, L. KSANFOMALITY, E. LELLOUCH, PH. MASSON, V. MOROZ, F. ROCARD, J. ROSENQVIST, C. SOTIN, AND A. SOUFFLOT 1990. ISM observation of Mars and Phobos. *Lunar Planet. Sci. Conf. 20th,* 461–471.

BINDER, A. B., AND J. C. JONES 1972. Spectrophotometric studies of the photometric function, composition and distribution of the surface materials of Mars. *J. Geophys. Res.* **77,** 3005–3020.

BURNS, R. G. 1992. *The Fate of Iron on Mars: Mechanism of Oxidation of Basaltic Minerals to Ferric-bearing Assemblages.* Workshop on Chemical Weathering on Mars, Lunar and Planetary Institute Technical Report 92-04, Part 1, pp. 8–9. [Abstract]

BURNS, R. G., AND D. S. FISHER 1993. Rates on oxidative weathering on the surface of Mars. *J. Geophys. Res.* **77,** 3365–3372.

CLARK, B. C., A. K. BAIRD, R. J. WELDON, D. M. TSUSAKI, L. SCHNABEL, AND M. P. CANDELARIA 1982. Chemical composition of the martian fines. *J. Geophys. Res.* **87,** 10059–10067.

ERARD, S., J.-P. BIBRING, J. MUSTARD, O. FORNI, J. W. HEAD, S. HURTEZ, Y. LANGEVIN, C. M. PIETERS, J. ROSENQVIST, AND C. SOTIN 1991. Spatial variations in composition of the Valles Marineris and Isidis Planitia regions of Mars derived from ISM Data. *Proc. Lunar Planet. Sci.* **21,** 437–455.

GEISSLER, P. E. 1992. *Spectrophotometric Mapping of Coprates Quadrangle, Mars.,* Ph.D. dissertation, Planetary Sciences Department, University of Arizona, Tucson.

GEISSLER, P. E., AND R. B. SINGER 1992. Spectrophotometric Mapping of Coprates Quadrangle, Mars. *Lunar and Planet. Sci. XXIII,* 403–404. [Abstract]

GILLESPIE, A. B., A. B. KAHLE, AND R. E. WALKER 1986. Color enhancement of highly correlated images. I. Decorrelation and HSI contrast stretches. *Rem. Sens. Environ.* **20,** 209–235.

GOODING, J. L. 1978. Chemical weathering on Mars: Thermodynamic stabilities of primary minerals (and their alteration products) from mafic igneous rocks. *Icarus* **33,** 483–513.

GOODING, J. L., R. E. ARVIDSON, AND M. YU 1992. Zolotov, physical and chemical weathering. In *Mars* (H. H. Kieffer, B. M. Jakosky, C. W. Snyder, and M. S. Mathews, Eds., pp. 626–651. Univ. of Arizona Press, Tucson.

HUGUENIN, R. L., J. B. ADAMS, AND T. B. MCCORD 1977. Mars: Surface mineralogy from reflectance spectra *Lunar Sci. VIII,* 478–480. [Abstract]

KLAASEN, K. P., T. E. THORPE, AND L. A. MORABITO 1977. Inflight performance of the Viking visual imaging subsystem. *Appl. Optics* **16,** 3158–3170.

KOCHEL, R. C., AND J. F. PIPER 1986. Morphology of large valleys on Hawaii: Evidence for groundwater sapping and comparisons with martian valleys. *J. Geophys. Res.* **91,** 175–192.

KOMATSU, G., P. E. GEISSLER, R. G. STROM, AND R. B. SINGER 1993. Stratigraphy and erosional landforms of layered deposits in Valles Marineris, Mars. *J. Geophys. Res.* **98, E6,** 11,105–11,121.

LUCCHITTA, B. K. 1990. Young volcanic deposits in the Valles Marineris, Mars. *Icarus* **86,** 476–509.

LUCCHITTA, B. K., G. D. CLOW, P. E. GEISSLER, A. S. MCEWEN, R. A. SCHULTZ, R. B. SINGER, AND S. W. SQUYRES 1993. The canyon system on Mars. In *Mars* (H. H. Kieffer, B. M. Jakosky, C. W. Snyder, and M. S. Mathews, eds., pp. 453–492. Univ. of Arizona Space Science Series, Tucson, AZ.

MALIN, M. C., G. E. DANIELSON, A. P. INGERSOLL, H. MASURSKY, J. VEVERKA, M. A. RAVINE, AND T. A. SOULANILLE 1992. Mars observer camera. *J. Geophys. Res.* **97,** 7699–7718.

MCCORD, T. B., AND J. B. ADAMS 1969. Spectral reflectivity of Mars. *Science* **163,** 1058–1060.

MCCORD, T. B., AND J. A. WESTPHAL 1971. Mars: Narrowband photometry, from 0.3 to 2.5 microns, of surface regions during the 1969 opposition. *Astrophys. J.* **168,** 141–153.

MCEWEN, A. S. 1992. Temporal variability of the surface and atmosphere of Mars: Viking orbiter color observations. *Lunar and Planet. Sci. XXIII,* 877–878. [Abstract]

MORRIS, R. V., H. V. LAUER, C. A. LAWSON, E. K. GIBSON, G. A. NACE, AND C. STEWART 1985. Spectral and other physicochemical properties of submicron powders of hematite, maghemite, magnetite, goethite and lepidocrocite. *J. Geophys. Res.* **90,** 3126–3144.

MORRIS, R. V., D. G. SCHULZE, H. V. LAUER, D. G. AGRESHI, AND T. D. SHELFER 1992. Reflectivity (visible and near IR) Mossbauer, static magnetic, and X-ray diffraction properties of aluminum-substituted hematite. *J. Geophys. Res.* **97,** 10257–10266.

MURCHIE, S. L., J. F. MUSTARD, J. BISHOP, J. W. HEAD, C. M. PIETERS, AND S. ERARD 1993. Spatial variations in the spectral properties of bright regions on Mars. Submitted for publication.

MUSTARD, J. F., S. ERARD, J-P. BIBRING, J. W. HEAD, S. HURTREZ, Y. LANGEVIN, C. M. PIETERS, AND C. J. SOTIN 1993. The surface of Syrtis Major: Composition of the volcanic substrate and mixing with altered dust and soil. *J. Geophys. Res.* **98,** 3387–3400.

NEDELL, S. S., S. W. SQUYRES, AND D. W. ANDERSON 1987. Origin and evolution of the layered deposits in the Valles Marineris, Mars. *Icarus* **70,** 409–411.

PLESCIA, J. B., AND R. S. SAUNDERS 1982. Tectonic history of the Tharsis region, Mars. *J. Geophys. Res.* **87,** 9775–9791.

SCHWERTMANN, U., AND R. M. TAYLOR 1989. Iron oxides. In *Minerals in Soil Environments* (J. B. Dixon, and S. B. Weed, eds.), pp. 379–438. Soil Society of America, Madison, WI.

SHARP, R. P. 1973. Mars: Troughed terrain. *J. Geophys. Res.* **78,** 4063–4072.

SHERMAN, D. M., R. G. BURNS, AND V. M. BURNS 1982. Spectral characteristics of the iron oxides with applications to the Martian bright region mineralogy. *J. Geophys. Res.* **87,** 10169–10180.

SHERMAN, D. M., AND T. D. WAITE 1985. Electronic spectra of Fe3+ oxides and oxide hydroxides in the near-IR to near-UV. *Am. Mineral.* **70,** 1262–1269.

SINGER, R. B. 1980. The dark materials on Mars. 1. New evidence from reflectance spectroscopy of the extent and mode of oxidation. *Lunar and Planet. Sci. XI,* 1048–1050. [Abstract]

SINGER, R. B. 1982. Spectral evidence for the mineralogy of high-albedo soils and dust on Mars. *J. Geophys. Res.* **87,** 10159–10168.

SINGER, R. B. 1985. Spectroscopic observation of Mars. *Adv. Space Res.* **5**(8), 59–68.

SINGER, R. B., AND J. S. MILLER 1991. Evidence for crystalline hematite as an accessory phase in Martian soils. *Proc. Mars Surf Atmosphere Through Time,* 134–135. [Abstract]

SINGER, R. B., AND H. Y. MCSWEEN 1993. The composition of the martian crust: Evidence from remote sensing and SNC meteorites. In *Resources of Near-Earth Space.* Univ. of Arizona Press, Tucson.

SODERBLOM, L. A. 1992. The composition and mineralogy of the martian surface from spectroscopic observations: 0.3 to 50 microns. In *Mars* (H. H. Kieffer, B. M. Jakosky, C. W. Snyder, and M. S. Mathews, eds.), Univ. Arizona Press, Tucson.

SODERBLOM, L. A., AND D. B. WENNER 1978. Possible fossil H_2O liquid–ice interfaces in the martian crust. *Icarus* **34,** 622–637.

THORPE, T. E. 1976. The Viking Orbiter cameras' potential for photometric measurement. *Icarus* **27,** 229–239.

TOWNSEND, T. E. 1987. Discrimination of iron alteration minerals in visible and near-infrared reflectance data. *J. Geophys. Res.* **92,** 1441–1454.

United States Geological Survey (USGS) 1988. *Planetary Image Cartography System.* Flagstaff, AZ

WITBECK, N.E., K. L. TANAKA, AND D. H. SCOTT 1991. *Geologic Map of the Valles Marineris Region of Mars, scale 1:2,000,000.* USGS Misc. Inv. Series Map I-2010.